JOURNAL OF MATERIALS SCIENCE LETTERS 24 (1989) 4152–4159

Diffusion bonding of grey cast iron to ARMCO iron and a carbon steel

F. A. CALVO, A. UREÑA, J. M. GOMEZ DE SALAZAR, F. MOLLEDA
Departamento de Ciencia de los Materiales e Ingeniería Metalúrgica, Facultad de Ciencias Químicas, Universidad Complutense de Madrid, Spain

The microstructure transformations produced during the diffusion bonding of grey cast iron to pure iron (ARMCO iron) and to a hypoeutectic steel (0.55% C) have been studied. The indirect determination of the carbon concentration profiles has produced a diffusion equation that relates the microstructure of the bond interface to the bonding temperature and time. A new tensile test specimen is described; this specimen has a variable circular section which allows the determination of true tensile strength of dissimilar diffusion bonds. Metallographic and fractographic studies have shown that the optimum bonding conditions for both types of joint are a bonding temperature at 980° C, for 5 min at a bonding pressure of 4.5 MPa.

1. Introduction

Welding of high carbon steels presents many problems when a conventional fusion welding technique is used. These problems increase if a grey cast iron is used, due to the high carbon and sulphur contents. These elements produce complex, hard and brittle heat-affected zones [1].

Diffusion bonding is a solid phase process [2, 3] that avoids many of the welding problems because it reduces the chemical, mechanical and structural heterogeneities associated with fusion welding. Diffusion bonding solves many of the problems that fusion welding methods present in the joining of grey cast iron, especially in dissimilar joints. The presence of carbon in the form of graphite produces important microstructure transformations that do not appear in similar [4–6] or dissimilar [7, 8] diffusion bonds of others iron alloys.

Using the classical laws of the intersticial diffusion, many of the microstructural transformations that occur during the diffusion bond trials can be predicted and a theoretical equation may be obtained that relates the bonding parameters (time and temperature) to the carbon penetration.

Our previous works [9, 10] have shown the microstructural transformations occurring during the diffusion bonding of ARMCO iron to carbon steel below the austenite range (A_3 temperature). The present work completes the previous research by using different ferrous alloys.

2. Experimental procedure

2.1. Materials and preparation

Parent materials used in the present work were ARMCO iron, BS: 979 (Part 1 1983) – En 9 080M40 carbon steel, and BS: 1452 – Grade 12 grey cast iron, whose chemical compositions are given in Table I.

The specimens to be bonded were in the form of cylinders 15 mm diameter and 5 and 35 mm long. The surfaces were ground with 600 grade silicon carbide paper and polished with a fine α-alumina to obtain an average roughness of 0.1 μm. The ground surfaces were ultrasonically cleaned.

2.2. Diffusion bonding conditions

Diffusion bonding was carried out in a vacuum of 10^{-3} Pa, at temperatures of 880 and 980° C, with a bonding time between 2 and 60 min. The bonding pressure was varied from 0.0 to 4.5 MPa. The parent materials were bonded to produce two dissimilar joints: ARMCO iron/cast iron and steel/cast iron. The equipment used to produce these bonds was described in a previous paper [11].

The short samples were prepared using conventional metallographic techniques and studied using both optical and electron optical techniques.

The long samples (70 mm length) were machined to make tensile test pieces.

2.3. Tensile test pieces

Two types of tensile test pieces were used: a standard parallel piece (BS: 18) with circular cross-section, nominal diameter 4 mm and length 29 mm (Type A); and a non-standard one, with a variable circular cross-section with a minimum diameter of 4 mm at the bond plane position (Type B) (Fig. 1).

Tensile testing using Type A specimen was not valid as the strength of the bond is higher than the cast iron; thus the failure always occurred in the parent material. Although some authors [12] consider the strength of

TABLE I Chemical composition of parent alloys

Materials	Elements (wt %)				
	C	Si	Mn	P	S
ARMCO iron	0.004	0.001	0.03	0.004	0.007
Carbon steel	0.55	0.25	0.65	0.03	0.03
Cast iron	3.55	2.25	0.50	0.40	0.10

0022–2461/89 $03.00 + .12

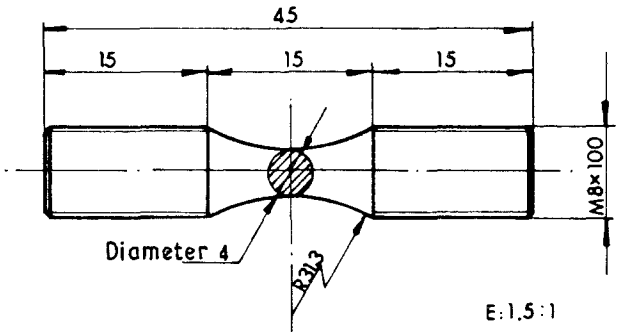

Figure 1 Tensile test piece: Type B.

this material as the tensile strength of the joint, the true tensile strength of diffusion bonds cannot be measured with standard cylindrical test pieces.

Type B test piece was used to determine the valid bond tensile strength. In this case the applied stress changes along the test piece and has a maximum value in the bond plane. This ensures that failure occurs close to the bond interface.

Both type A and B specimens were tested in an Instron test machine at a cross-head speed of 0.01 mm min^{-1}.

3. Results

3.1. Microstructure of diffusion-bonded joints

Metallographic study showed that a rapid diffusion of carbon occurs from the cast iron to the ARMCO iron or the steel. This diffusion causes the formation of a carbon-rich zone in these materials, and a decarburization zone in the cast iron close to the bond interface (Figs 2a and b).

The carbon-rich zone in the ARMCO iron/cast iron joints has a typical ferritic/pearlitic microstructure with carbon contents that change gradually with distance from the bond interface. Carbon contents can be

TABLE II Thickness of diffusion layers formed during diffusion bonding of ARMCO iron to cast iron

Specimen	T_b (°C)	t_b (min)	Diffusion layer thickness (μm)		
			Carbon-rich zone		Spheroidization zone
			A	B	
HF_1	980	60	1000	–	160
HF_2	980	40	700	–	130
HF_3	980	30	600	–	110
HF_4	980	20	500	–	80
HF_5	980	10	350	–	60
HF_6	880	30	500	550	90
HF_7	880	20	400	400	70
HF_8	880	10	250	250	50

A: ferritic/perlitic zone.
B: carbide precipitation zone.
(A + B): carbon-rich zone.

in excess of 0.8% near the bond interface when both materials are bonded at 980° C for more than 20 min. In these cases, proeutectic cementite is formed at grain boundaries in contact with the bond interface (Fig. 3).

Unless the bonding temperature is higher than 880° C the interfacial defects (voids) are not eliminated and the original bond interface is still apparent (Fig. 4). It is believed that the operative mechanisms are similar to those proposed by King and Owczarski [13, 14] to explain joint formation during diffusion bonding of pure titanium.

It has been shown that when the bonding temperature is lower than 910° C (A_3 temperature for pure iron) carbide precipitation in the ferrite takes place close to the carbon-rich zone. This zone is not observed in joints bonded at 980° C, due to the supersaturation of carbon in the Fe-α matrix (Fig. 5). The formation process of these carbides (ε and cementite) is similar to that observed by the present authors [9] during the diffusion bonding of ARMCO iron to carbon steel at 900° C.

The thickness of each diffusion zone depends on bonding variables, and generally increasing time and temperature produces a larger zone. However, it has been observed that the penetration distance of carbon in pure iron is greater at 880° C than at 980° C due to the formation of the precipitation zone. The thickness of the diffusion zones for iron/cast iron joints bonded at different temperatures and times is shown in Table II.

The carbon-rich zone formed in steel/cast iron joints has a higher carbon content than in the

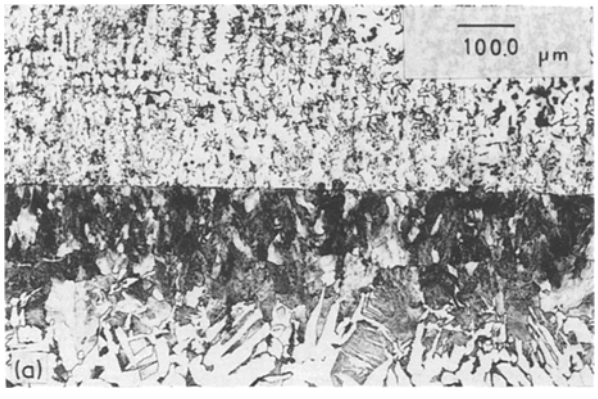

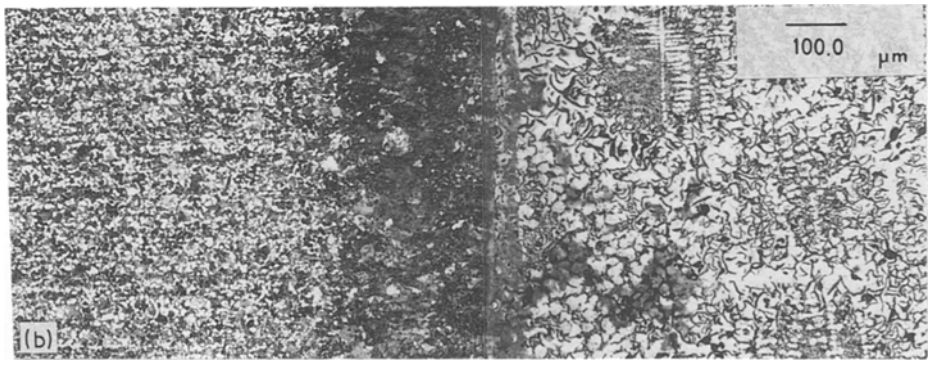

Figure 2 (a) ARMCO iron/cast iron diffusion-bonded joint (T_b = 880° C, t_b = 20 min, P_s = 4.5 MPa) × 72. (b) 0.55% C steel/cast iron diffusion-bonded joint (T_b = 980° C, t_b = 10 min, P_b = 4.5 MPa) × 72.

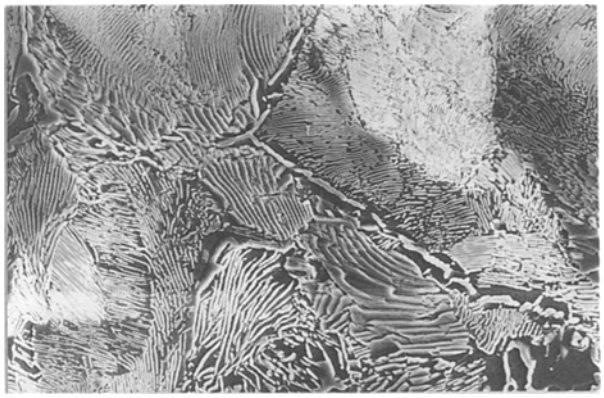

Figure 3 Proeutectic cementite in the grain boundaries of the carburation zone of ARMCO iron (T_b = 980° C, t_b = 60 min, P_b = 4.5 MPa).

ARMCO/cast iron case. A wide diffusion layer with a typical microstructure of a hypereutectic steel (> 0.8% C) is formed close to the bond interface, even when the bond is formed at 880° C (Fig. 6). In joints bonded at 980° C with bonding times > 30 min, the carbon content in the steel close to the interface can be higher than the solubility limit for carbon in austenite at the bonding temperature (~ 1.5%). When this occurs, graphite nodule precipitation is observed (Fig. 7). The nucleation of this graphite occurs on the proeutectic cementite/austenite interfaces. The growth mechanisms of the graphite nodules are similar to these proposed by Hussein *et al.* [15].

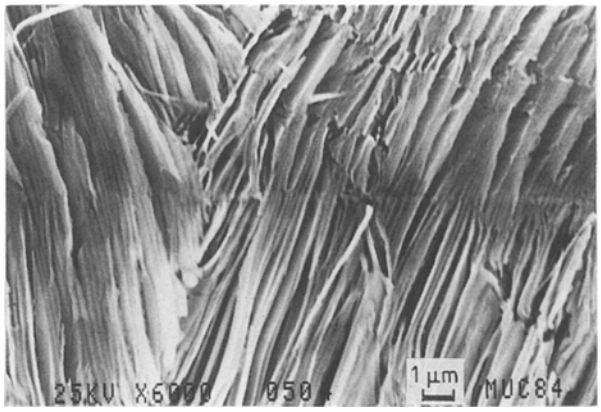

Figure 4 Diffusion bonded joint between ARMCO iron and cast iron at 980° C, 45 min and 4.5 Pa.

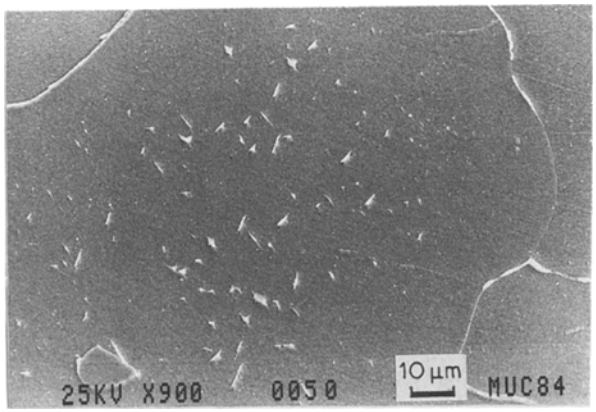

Figure 5 Precipitation of iron carbides in ferrites in a diffusion-bonded joint between ARMCO iron and cast iron (T_b = 880° C, t_b = 20 min, P_b = 4.5 MPa).

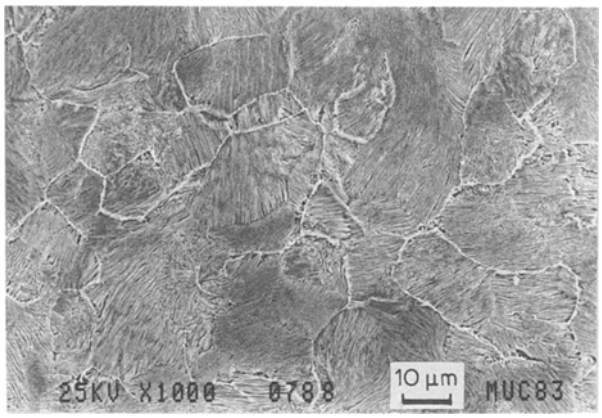

Figure 6 Hypereutectoid steel formed in the carburation zone of a steel/cast iron diffusion bond (T_b = 980° C, t_b = 20 min, P_b = 4.5 MPa).

The diffusion bonding of carbon steel to cast iron in the temperature range studied is always carried out over the A_3 temperature. For this reason the change in the bonding temperature between 880 and 980° C does not produce substantial microstructural modifications in the parent steel, and the elimination of the original interface has been also observed in joints bonded at 880° C. The increase of bonding time only produces an increase of the diffusion layer thickness (Table III).

However, the most interesting transformations occur in the decarburarization zone of the cast iron in both the ARMCO iron/cast iron and steel/cast iron joints. The diffusion of carbon into ARMCO iron (or steel) favours the partial dissolution of graphite flakes

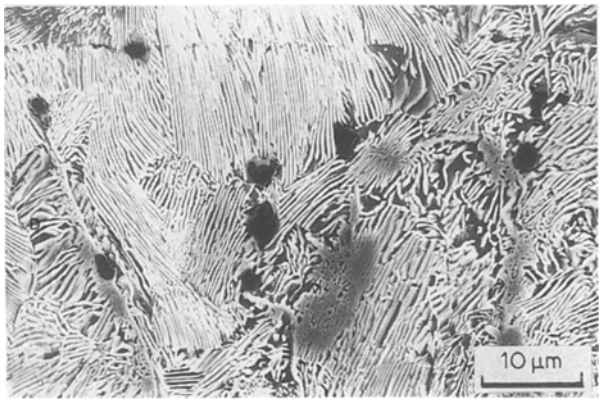

Figure 7 Graphite nodules precipitated in the rich carbon zone of the steel (T_b = 980° C, t_b = 30 min, P_b = 4.5 MPa).

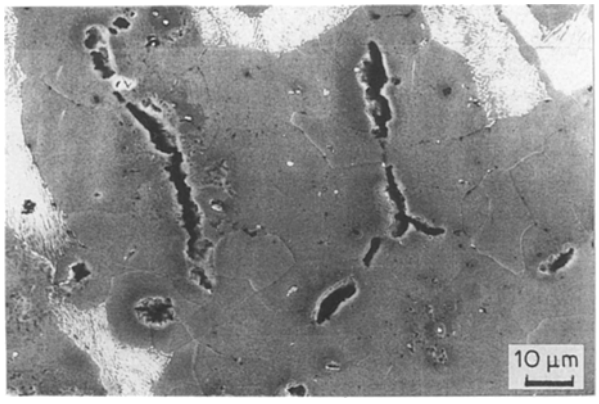

Figure 8 Break-up of graphite flakes.

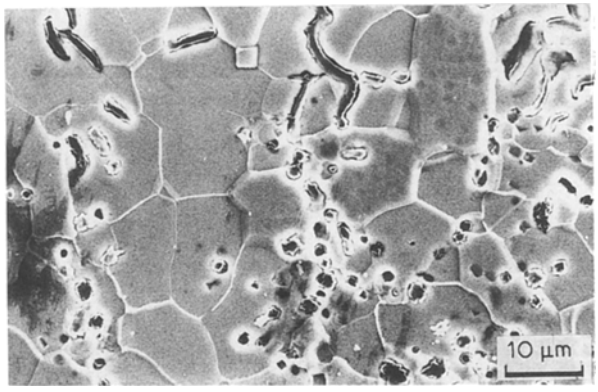

Figure 9 Spheroidization of graphite flakes.

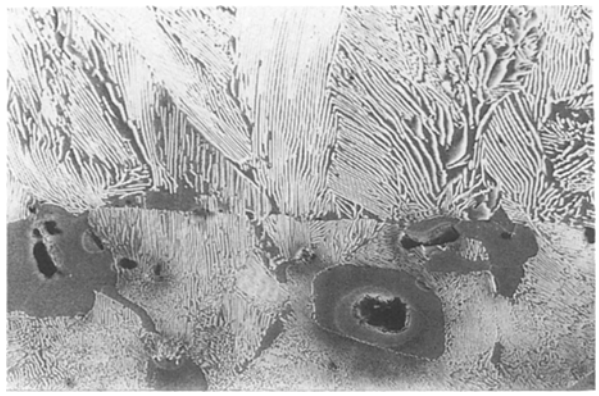

Figure 10 Ferritic shells surrounding graphite nodules.

during bonding. It has been observed that this dissolution does not occur at the same speed on all the flake surfaces (Fig. 8). This causes the break-up of the flakes and their spheroidization to obtain less energetic morphologies (Fig. 9). This phenomenon is very similar to the dissolution process observed with primary silicon crystals in Al–Si alloys during spheroidization heat treatments [16].

The process of break-up and spheroidization depends on the temperature and bonding time, where an increase can produce the complete dissolution of the graphite flakes closest to the bond interface. This instigates an increase of the carbon content in the austenitic matrix of the cast iron that produced a perlitic matrix during the cooling. It has been

TABLE III Thickness of diffusion layers formed during diffusion bonding of steel to cast iron

Specimen	T_b (°C)	t_b (min)	Diffusion layer thickness (μm)	
			Carbon-rich zone	Spheroidization zone
AF_1	980	60	1000	200
AF_2	980	40	800	175
AF_3	980	30	650	150
AF_4	980	20	400	100
AF_5	980	10	500	50
AF_6	880	30	400	100
AF_7	880	20	250	75
AF_8	880	10	250	50

observed that when this phenomenon occurs, the undissolved graphite nodules undergo a coarsening process and become surrounded by "ferrite shells" (Fig. 10), due to the carbon diffusion from the surrounding austenite matrix [17].

An increase in the bonding pressure improves the contact between the bonded surfaces and produces several important differences in behaviour. These are an increase of the break-up and spheroidization phenomena and an increase of thickness of the carbon-rich zone (Figs 11a and b).

3.2. Determination of carbon concentration profiles

Quantitative metallography was applied to determinate the carbon concentration profiles of the ARMCO iron/cast iron and steel/cast iron using the relationship

$$\% \text{ carbon} \approx 0.8 \times (\% \text{ perlite}) \times 100$$

Figs 12a and b show two of these experimental profiles (discontinuous lines) determinated for two joints bonded at 980° C for 60 min.

These experimental profiles at 980° C may be compared with those obtained for the carbon diffusion into a semi-infinite bar with a constant carbon surface concentration. This is the normal case in the carburization process of a steel. Using Fick's second law with the boundary conditions

$$C(x = 0) = C_s \quad \text{and} \quad C(x = \infty) = C_o \quad (1)$$

where C_s is the surface concentration and C_o the original carbon concentration of the steel (or iron)

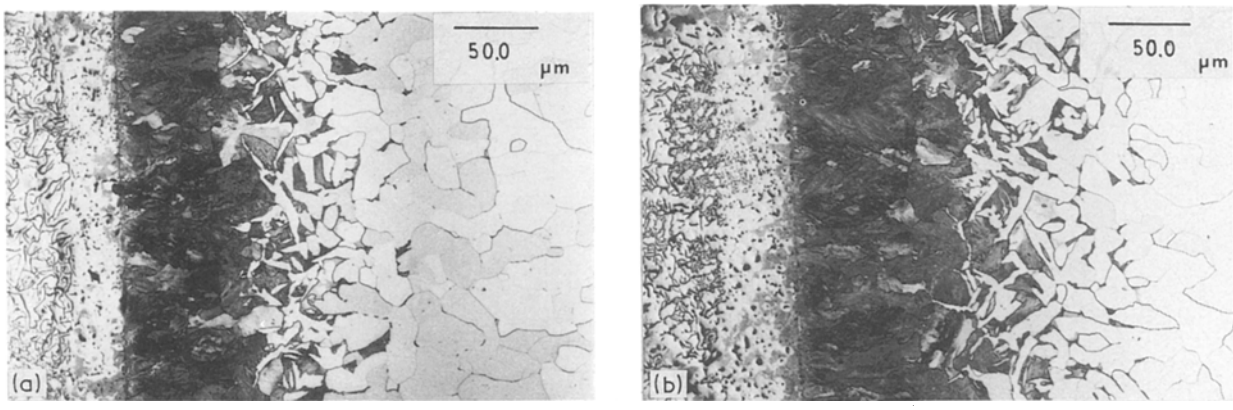

Figure 11 Effect of the bonding pressure on the diffusion layer. (a) T_b = 980° C, t_b = 2 min, P_s = 1.0 MPa, and (b) T_b = 980° C, t_b = 2 min, P_b = 4.5 MPa.

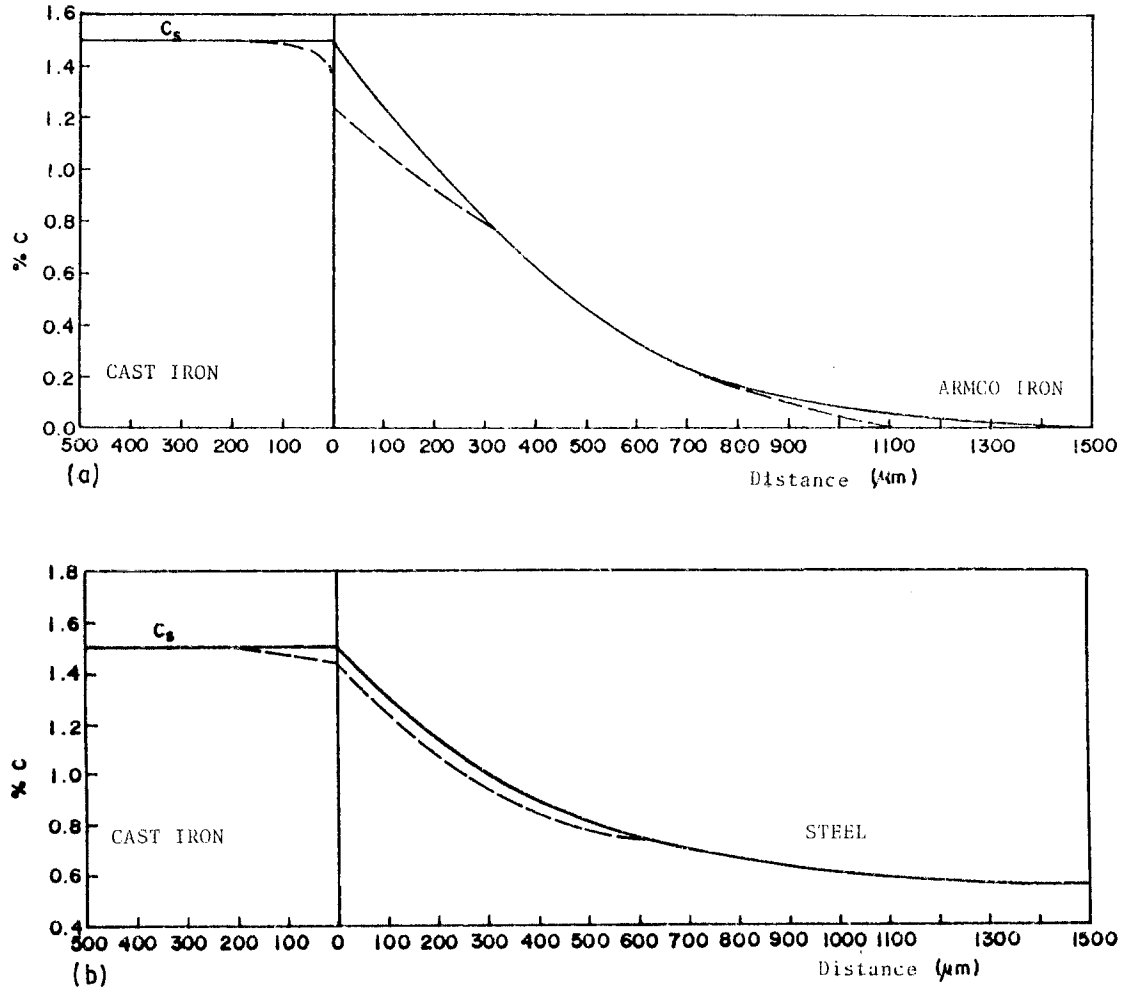

Figure 12 (a) Carbon concentration profile in a ARMCO iron/cast iron diffusion bond. (T_b = 980° C, t_b = 60 min, P_b = 4.5 MPa). (b) Carbon concentration profile in a steel/cast iron diffusion bond (T_b = 980° C, t_b = 60 min, P_b = 4.5 MPa). (——) Theoretical, (- - -) experimental curves.

[18, 19] we have

$$C = C_s - (C_s - C_o) \operatorname{erf}\left[\frac{x}{2(Dt)^{1/2}}\right] \quad (2)$$

For carbon diffusion in austenite at 980° C, D is 3.5×10^{-11} m sec^{-1} [20]. The equation therefore reduces in the present case to

$$C = C_s - (C_s - C_o) \operatorname{erf} \frac{x}{5.9 \times 10^{-6} t^{1/2}} \quad (3)$$

where C_s is the equilibrium concentration in the austenite matrix of cast iron at the bonding temperature,

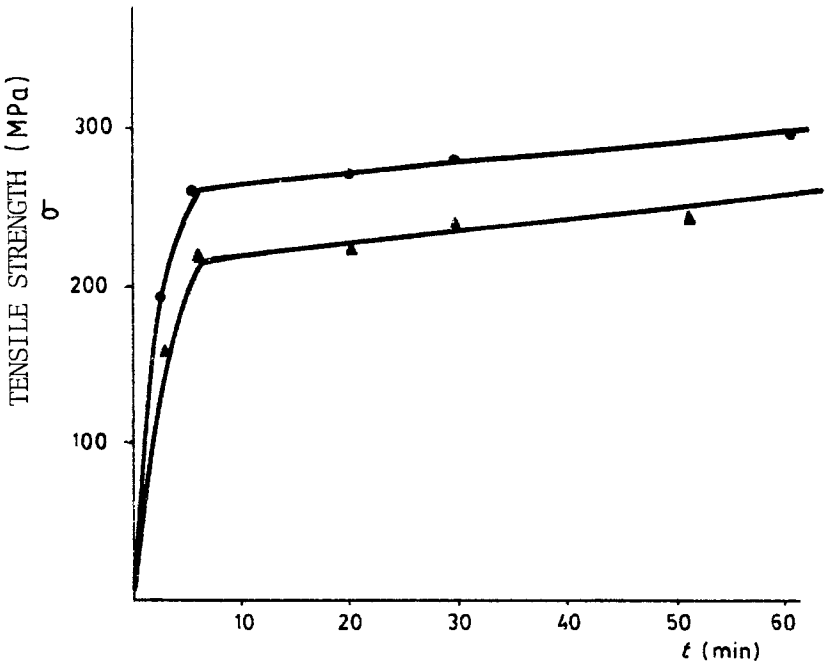

Figure 13 Effect of the tensile strength of Type B diffusion bonds: (●) steel–cast iron, (▲) ARMCO iron–cast iron.

C_0 the original carbon concentration in either the iron or the steel, x the distance to the bond interface, t the bonding time, T the bonding temperature and erf the error function. The results from Equation 3 are plotted in Figs 12a and b and indicate a close similarity with the experimental results. This supports the diffusion controlled mechanisms being proposed.

3.3. Tensile test

Tensile tests with Type A specimens showed that the tensile strength of both joints is higher than the strength of the cast iron for bonding times longer than 5 min and temperatures of 980° C. However, this type of test piece did not allow determination of the true strength when the bonding times were greater than 5 min.

Using Type B specimens, where the failure always occurs through the bond interface, it was shown that the bond strength increased with the bonding time.

The tensile strengths obtained for the ARMCO iron/cast iron and steel/cast iron joints bonded at 980° C, 5 min, and 4.5 MPa, are 215 and 250 MPa, respectively. Both values are higher than the tensile strength of the parent cast iron (~ 190 MPa) (Fig. 13).

Increase of the bonding time above 5 min produces a small increase in the tensile strength of both joints, this increase being related to the spheroidization of the graphite flakes in the cast iron. The maximum strengths after 60 min were 255 and 290 MPa, respectively. These values are closer to those reported for a nodular cast iron with ferritic matrix [20].

For bonding times shorter than 5 min, the tensile strength of both joints was always less than 200 MPa.

3.4. Fractography

The SEM observations of the fracture surfaces associated with the Type B samples do not show any significant differences between the different joints. This arose because the failure occurred in the spheroidization zone of the cast iron. The fracture surfaces of both joints are brittle, although an increase in the bonding time (> 30 min) produces an increase in the ductile behaviour.

Three different fracture morphologies have been distinguished in these samples.

(i) Type I failure. This failure preferentially occurs across the original bond plane, and only few isolated bonded points are observed. At these points the intergranular and brittle failure always occurs in the parent cast iron (Fig. 14). The failure begins as cracks that nucleate at the end of the graphite flakes (Fig. 15). This type of failure appears in samples bonded for less than 5 min.

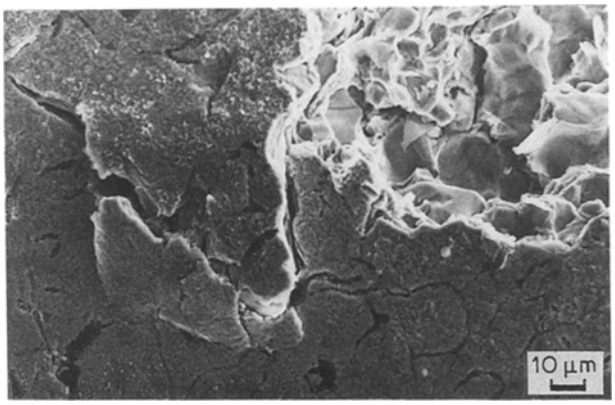

Figure 15 Intergranular fracture of the cast iron side.

(ii) Type II failure. The original bond surface could still be observed, but several transformations were produced. As Fig. 16 shows, there is an increase in ductile behaviour, and partial spheroidization of the graphite flakes that are in contact with the iron (or steel) surface. The ductile fracture zones are lightly dimpled and coincide with the zone of austenite/austenite contact. However, the fracture in the zone of austenite/graphite contact is brittle and no changes are observed on the polished surface of the ARMCO iron (Fig. 16).

(iii) Type III failure. The fracture surface is no longer planar and failure is toward the spheroidization zone of the graphite. The fracture morphology depends on the spheroidization grade of the graphite flakes (Fig. 17). Even, quasicleavage fracture zones have been observed in ARMCO iron-cast iron joints bonded during long times.

In general, Type I and II failure are predominant in bonds with low to average strength (< 200 MPa) that were bonded for less than 5 min; whilst Type III failure was observed in the bond with a tensile fracture strength > 200 MPa.

4. Discussion

Results have shown that temperature controls the

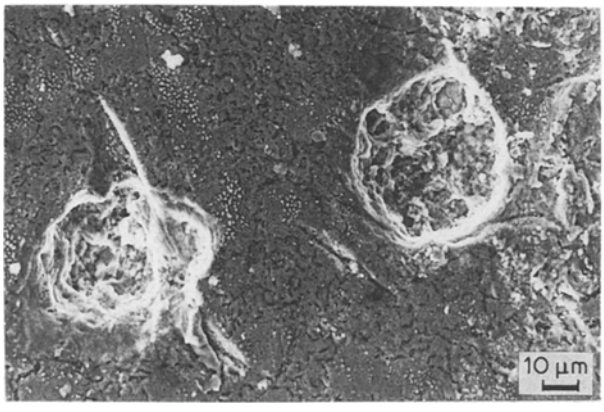

Figure 14 Fracture surface in a steel–cast iron joint bonded at 980° C, 2 min and 4.5 MPa. Failure Type 1: cast iron side.

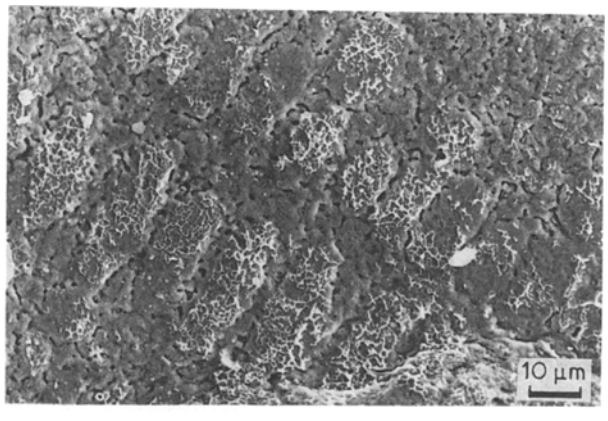

Figure 16 Failure Type 2 in a ARMCO iron/cast iron joint bonded at 980° C, 4 min and 4.5 MPa: cast iron side.

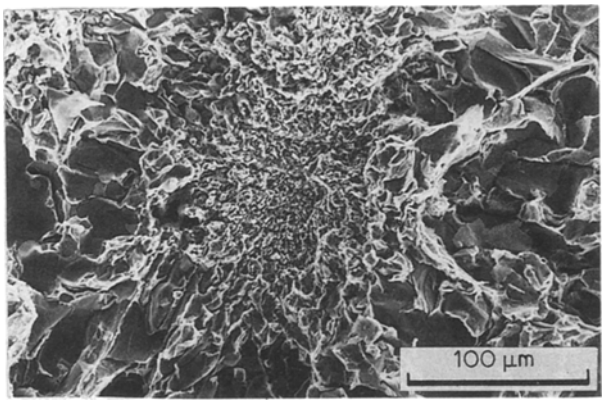

Figure 17 Failure Type 3 in a steel/cast iron joint bonded at 980° C, 20 min and 4.5 MPa.

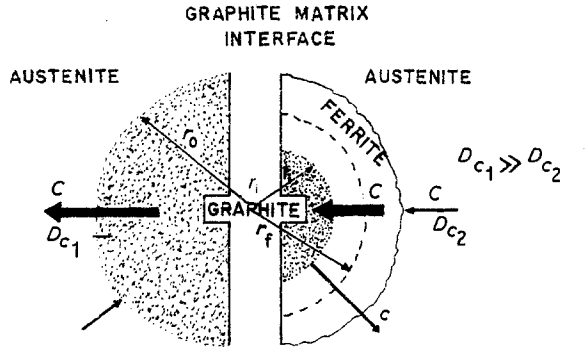

Figure 18 Formation mechanism of ferritic shells around the graphite nodules in the cast iron. r_0 = graphite nodule size at the beginning of the spheroidization process, T_b; r_i = graphite nodule size at the end of the spheroidization process, T_b; r_f = graphite nodule size at room temperature.

microstructure transformations that occur during the diffusion bonding of a grey cast iron to iron or carbon steel. It has been observed that only when the bonding temperature is higher than the A_3 temperature is the bond interface eliminated. This is due to recrystallization and again grain growth of austenite across the bond interface. This mechanism explains the differences observed in the diffusion bond of ARMCO iron to cast iron at 880° C in relation to the specimens bonded at 980° C. As the A_3 temperature is 910° C, diffusion bonding at 880° C will mean that an austenitic matrix (cast iron) and a ferritic matrix (ARMCO iron) are in contact. It explains the precipitation of iron carbides in ferrite and the absence of recrystallization across the bond interface.

As carbon diffusion in α-Fe is faster than in γ-Fe even at lower temperatures ($D_c = 1.5 \times 10^{-10}$ m^2 sec^{-1} at 880° C and $D_c = 3.6 \times 10^{-11}$ m^2 sec^{-1} at 980° C) [21], the greater penetration distance of carbon in ARMCO iron at 880° C than at 980° C, can be explained. However, both time and bonding pressure play important roles in the joint formation. Bonding time, together with temperature, controls the thickness of the diffusion layer (carbon-rich and graphite spheroidization zones). Bonding pressure accelerates the break up of graphite flakes. The studies of Plenard and Fromont [22] on malleable cast iron subjected to axial compression during heat treatments, show that increasing pressure favours the subdivision of the graphite nodules. These authors attribute this phenomenon to increases in dislocation and microcrack density. This increase defect concentration can then act as preferential places for the nucleation of the graphite nodules.

The dissolution of graphite in the austenitic matrix allows the carbon concentration in it to remain constant during the bonding, thus balancing the diffusion towards the iron or steel. This allows the use of a constant surface potential model where it is considered that the carbon concentration in the surface of the "carburizing" material is maintained constant. This constant value is the solubility limit of carbon in austenite at the bonding temperature.

The experimental observations show that graphite acts as a source of carbon during the diffusion bonding. However, the formation of ferritic shells around the graphite nodules in the spheroidization zone of the cast iron, shows that during the cooling the diffusion potential changes and the graphite nodules behave as "sinks" for carbon. This phenomenon produces the coarsening of these graphite nodules (Fig. 18).

The results obtained from tensile tests using Type B specimens shows that bonding for 5 min at 980° C and 4.5 MPa is enough to produce joints with tensile strengths greater than the parent cast iron.

5. Conclusions

1. The optimum bonding conditions for the diffusion bonding of a grey cast iron to a pure iron and to carbon steel are: $T_b = 980°$ C, $t_b = 5$ min and $P_b = 4.5$ MPa. The tensile strength of both joints bonded under these conditions were 215 and 250 MPa, respectively. Both values are higher than the nominal tensile strength of the as-received cast iron.

2. Temperature is the variable that controls the bond formation and it is necessary to bond above the A_3 temperature to eliminate the interfacial voids and for the bond interface to disappear.

3. Graphite flakes act as a source of carbon to the austenitic matrix that surrounds it. Their dissolution instigates the break-up and spheroidization.

4. During cooling, the direction of the carbon diffusion changes and the graphite nodules act as carbon sinks. This explains the formation of ferritic shells.

5. The high carbon contents that are reached in the carbon-rich zone of steel–cast iron joints bonded at 980° C for more than 30 min, make possible the precipitation of carbon as graphite nodules in the steel.

6. An analytical expression obtained by solving Fick's second law can be applied to the diffusion bonding of grey cast irons to iron or steels.

References

1. J. F. LANCASTER, "Metallurgy of welding" (Allen and Unwin, London, 1987) p. 212.
2. P. M. BARTLE, *Weld. J.* **54** (1975) 799.
3. W. D. OWCZARSKI and D. F. PAULONIS, *ibid.* **60** (1981) 22.
4. B. DERBY and E. R. WALLACH, *J. Mater. Sci.* **19** (1984) 3149.
5. A. KYSOJIN, T. ITON and K. NISHIMOTO, *Bull. Jpn. Soc. Precis. Eng.* **13** (1979) 201.
6. S. ELLIOT, J. A. BUCKLOW and E. R. WALLACH, *J. Mater. Sci.* **15** (1980) 2823.
7. N. F. KAZAKOV, "Diffusion bonding of materials" (Pergamon, Oxford, 1985).

8. D. S. TAYLOR and C. POLLARD, in Proceedings of the International Conference, "Advances in Welding Processes" (The Welding Institute, Harrogate, 1978) p. 1.
9. F. A. CALVO, F. MOLLEDA, J. M. GOMEZ DE SALAZAR, A. J. CRIADO and J. C. SUAREZ, *Metallogr.* **19** (1986) 177.
10. F. A. CALVO, F. MOLLEDA, J. M. GOMEZ DE SALAZAR, A. J. CRIADO and A. UREÑA, *Rev. Soldadura* **16** (1986) 125.
11. F. A. CALVO, A. UREÑA, J. M. GOMEZ DE SALAZAR, F. MOLLEDA and A. J. CRIADO, *J. Mater. Sci.* **23** (1988) 1231–1236.
12. T. ENJO, M. IKEUCHI, M. KANAJ and T. MARUYAMA, *Trans. Jpn Welding Res. Inst.* **6** (1977) 123.
13. W. H. KING and W. A. OWCZARSKI, *Welding J. Res. Suppl.* (1967) 2895–2985.
14. *Idem, ibid.* **47** (1968) 444s.
15. A. A. HUSSEIN, L. I. EL-MENAWATI, M. A. KASSEN and B. J. YOTOS, in Proceedings of the Conference Symposium, "The Physical Metallurgy of Cast Iron", edited by H. Fredrikson and M. Hillert (North-Holland, New York, 1984) pp. 3–5.
16. F. A. CALVO, A. J. CRIADO, J. M. GOMEZ DE SALAZAR and F. MOLLEDA, *Rev. Metallurgia* **21** (1985) 342.
17. B. LUX, F. MOLLARD and I. MINKOFF, in Proceedings of the Conference, 2nd International Symposium, "Metallurgy of Cast Iron", edited by B. Lux, I. Minkoft and F. Mollard (Georgi, Switzerland, 1975) p. 371.
18. J. CRANK, "The Mathematics of Diffusion" (Oxford University Press, Oxford, 1956).
19. D. A. PORTER and K. A. EASTERLING, "Phase Transformations in Metals and Alloys" (Van Nostrand Reinhold, UK, 1981) p. 73.
20. ASM, "Metal Handbook", 9th Edn, Vol. 1 edited by Bruce P. Bardes (ASM, Metals Park, Ohio, 1978) p. 35.
21. R. W. K. HONEYCOMBE, "Steels, Microstructure and Properties" (Edward Arnold, London, 1982) p. 7.
22. E. PLENARD and C. FROMOT, in Proceedings of the Conference Symposium "The Physical Metallurgy of Cast Iron", edited by H. Fredriksson and M. Millert (North-Holland, New York, 1984) p. 297.

Received 11 April 1988
and accepted 14 February 1989